

Strong-coupling corrections to Bardeen-Cooper-Schrieffer ratios

F. Marsiglio and J. P. Carbotte

Physics Department, McMaster University, Hamilton, Ontario, Canada L8S 4M1

(Received 9 August 1985; revised manuscript received 28 October 1985)

We have calculated simple approximate expressions for the normalized specific-heat difference between superconducting (S) and normal (N) states at and below T_c and for the ratio $\gamma T_c^2/H_c^2(0)$, using a square-well model for the gap. While our approach is very different, the formulas obtained have the same general form as those that have already appeared in the literature. Each contains two parameters, which we determine through a phenomenological fit to exact numerical results from Eliashberg theory. The strong-coupling variable is T_c/ω_{in} , where ω_{in} is the Allen-Dynes expression for the average phonon energy.

I. INTRODUCTION

The BCS theory¹ of superconductivity provides universal predictions for a number of ratios such as $2\Delta_0/k_B T_c$, $\gamma T_c^2/H_c^2(0)$, $\Delta C(T_c)/\gamma T_c$, etc. Here Δ_0 is the zero-temperature energy gap, T_c the critical temperature, γ the Sommerfeld constant, $H_c(0)$ the critical magnetic field at zero temperature, and $\Delta C(T_c)$ the specific-heat jump at T_c . When confronted with experimental results, the BCS predictions are found to be qualitatively correct, but quantitatively inaccurate.² Eliashberg theory,³ which includes retardation effects the electron-phonon interaction and deals with realistic kernels involving the material parameters of a given superconductor, has been found to be very accurate.⁴⁻¹⁰ Because of the complexity of the underlying equations, however, only numerical results can be obtained.

In a previous paper Mitrović *et al.*¹¹ considered the ratio of the gap to critical temperature ($2\Delta_0/k_B T_c$). First, they calculated $2\Delta_0/k_B T_c$ for a large number of superconductors from accurate numerical solutions based on known electron-phonon spectral densities $\alpha^2(\Omega)F(\Omega)$ previously determined by inversion of tunneling data. As a second step, they considered the Eliashberg equations written on the real frequency axis and generalized the original work of Leavens and Carbotte¹² to obtain an analytic formula for $2\Delta_0/k_B T_c$ with a strong-coupling correction. The approximations used to accomplish this, while reasonable, are not controlled and not necessarily completely consistent. To account for this, phenomenological parameters are introduced along the way and only the general form obtained is assumed to be significant. The general form is the same as that previously obtained by Geilikman and Kresin,¹³ who used very different methods and approximations. The resulting formulas of Mitrović *et al.*, once the two phenomenological parameters are chosen, are found to give a good semiquantitative fit to all the exact numerical values for $2\Delta_0/k_B T_c$. In most cases considered, the fluctuations from the general form are surprisingly small.

In this paper we wish to extend the work of Mitrović *et al.*¹¹ to other BCS ratios. We start with the Eliashberg equations written on the imaginary axis, and use approxi-

mations appropriate to the Matsubara representation specifically designed to generate analytic expressions (for the various ratios of interest) of the same general form as obtained by Geilikman and Kresin,¹³ Geilikman, Kresin, and Masharov,¹⁴ and Kresin and Parkhomenko.¹⁵ The undetermined constants that are introduced in the course of simplifying the algebra are fixed by consideration of exact numerical data based on the known $\alpha^2(\Omega)F(\Omega)$ for several materials. This procedure is done for each BCS ratio. While it will become clear that within our approximation scheme the unknown constants for different ratios are not independent, we treat them as such, since our initial approximation may be less accurate for one particular ratio than for another. As in Ref. 11, we only attempt, in our fit, to reproduce the general trend. While this can be done in a satisfactory way for each of the thermodynamic ratios considered, we find that the fluctuations from material to material are larger than previously found for $2\Delta_0/k_B T_c$. Still, in most cases, they are sufficiently small to make the resulting approximate formulas quite useful in analyzing experimental data. Of course, if more precision is desired it is necessary to solve numerically the full Eliashberg equations without approximation and to know the spectral density $\alpha^2(\Omega)F(\Omega)$ accurately.

In Sec. II we consider first the specific-heat jump at and near T_c . In Sec. III an alternate derivation of the strong-coupling corrections to the gap edge, starting with the Eliashberg equations on the imaginary axis, is given. This, in turn, leads to the correction for $\gamma T_c^2/H_c^2(0)$. Brief conclusions are contained in Sec. IV.

II. STRONG-COUPLING CORRECTION TO $\Delta C(T)/\gamma T_c$

We begin with the Eliashberg equations, written on the imaginary frequency axis³ ($k_B \equiv \hbar \equiv 1$),

$$\begin{aligned} \Delta(i\omega_n)Z_s(i\omega_n) &= \pi T \sum_{m=-\infty}^{\infty} [\lambda(n-m) - \mu^*(\omega_c)\Theta(\omega_c - |\omega_m|)] \\ &\quad \times \frac{\Delta(i\omega_m)}{[\omega_m^2 + \Delta^2(i\omega_m)]^{1/2}}, \end{aligned} \quad (1)$$

$$\omega_n Z_s(i\omega_n) = \omega_n + \pi T \sum_{m=-\infty}^{\infty} \lambda(n-m) \frac{\omega_m}{[\omega_m^2 + \Delta^2(\omega_m)]^{1/2}}, \quad (2)$$

where $\Delta(i\omega_n)$ are the gaps and $Z_s(i\omega_n)$ are the renormalization factors, defined at the Matsubara frequencies

$$i\omega_n = i\pi T(2n-1), \quad n=0, \pm 1, \pm 2, \dots \quad (3)$$

The electron-phonon spectral density $\alpha^2(\Omega)F(\Omega)$ appears through the relation

$$\lambda(n-m) = \int_0^{\infty} \frac{2\Omega\alpha^2(\Omega)F(\Omega)}{\Omega^2 + [2\pi T(n-m)]^2} d\Omega, \quad (4)$$

and $\mu^*(\omega_c)$ is the Coulomb pseudopotential with cutoff ω_c . Starting with the corresponding real frequency equations,⁴ Leavens and Carbotte¹⁶ have derived an approximate T_c equation. The same T_c equation can be derived from Eqs. (1) and (2) using the step-function approximation

$$\Delta(\omega_n) = \begin{cases} \Delta_0(T), & |\omega_n| < \omega_0 \\ \Delta_{\infty}(T), & |\omega_n| > \omega_0 \end{cases} \quad (5a)$$

$$Z_s(\omega_n) = \begin{cases} Z_0(T), & |\omega_n| < \omega_0 \\ 1, & |\omega_n| > \omega_0. \end{cases} \quad (5b)$$

Here ω_0 represents the maximum phonon frequency in the system. The advantage of the imaginary axis equations lies in the fact that they tend to reduce to simple expressions more systematically under an approximation such as (5). For T near T_c , we can expand Eqs. (1) and (2) and evaluate the left-hand sides for small n ($n=1$) and for $n \rightarrow \infty$. We restrict our spectra to those in which the important phonon frequencies are much higher than T_c and much less than ω_0 . The Coulomb cutoff ω_c is taken to be much larger than any other energy in the problem. This allows an expansion in the strong-coupling parameter T/Ω . The resulting solution for $\Delta_0(T)$ is given by

$$1 = F(T) = \Delta_0^2(T)G(T) + \Delta_0^4(T)J(T), \quad (6)$$

where

$$F(T) \equiv \frac{\lambda - \mu^*}{1 + \lambda} \ln \left[\frac{1.13\omega_0}{k_B T} \right] - \frac{\bar{\lambda}}{1 + \lambda} - \frac{(\pi T)^2}{1 + \lambda} \left[\bar{a}(T) - \frac{4}{3}\bar{b} \right], \quad (7a)$$

$$G(T) \equiv -\frac{7}{8} \frac{\lambda - \mu^*}{1 + \lambda} \frac{\zeta(3)}{(\pi T)^2} + \frac{1}{2(1 + \lambda)} \{ 3\bar{a}(T) + [\frac{7}{4}\zeta(3) - 1]\bar{b} \}, \quad (7b)$$

$$J(T) \equiv \frac{93}{128} \frac{\lambda - \mu^*}{1 + \lambda} \frac{\zeta(5)}{(\pi T)^4} - \frac{\bar{b}}{1 + \lambda} \frac{1}{(\pi T)^2} \left[\frac{63}{32}\zeta(3) + \frac{93}{128}\zeta(5) \right]. \quad (7c)$$

λ and $\bar{\lambda}$ are defined in Ref. 16. Strong-coupling corrections are expressed in terms of two moments of the spectral density function,

$$\bar{a}(T) \equiv \int_0^{\infty} d\Omega \frac{2\alpha^2(\Omega)F(\Omega)}{\Omega^3} \ln \left[\frac{1.13\Omega}{k_B T} \right], \quad (8a)$$

$$\bar{b}(T) \equiv \int_0^{\infty} d\Omega \frac{2\alpha^2(\Omega)F(\Omega)}{\Omega^3}. \quad (8b)$$

$\zeta(N)$ is the Riemann zeta function. Note that terms of order Ω/ω_0 have been neglected.

To calculate the specific-heat jump, we use the Bardeen-Stephen formula for the free energy,^{17,18}

$$\frac{\Delta F}{N(0)} = -\pi T \sum_{m=-\infty}^{\infty} \{ [\omega_m^2 + \Delta^2(m)]^{1/2} - |\omega_m| \} \times \left[Z_s(m) - Z_N(m) \times \frac{|\omega_m|}{[\omega_m^2 + \Delta^2(m)]^{1/2}} \right]. \quad (9)$$

We use $Z_N(m) = 1 + \lambda$ and ignore the m dependence in the logarithm in $Z_s(m)$ so that the sum can be performed analytically. The result is

$$\frac{\Delta F}{N(0)} = \frac{1}{2} \frac{(1 + \lambda)^2}{\lambda - \mu^*} [\Delta_0^4(T)K(T) + \frac{4}{3}\Delta_0^6(T)L(T)], \quad (10)$$

where

$$K(T) \equiv G_0(T) - \frac{TF'_0(T)}{1 + \lambda} \left[\bar{c}(T) - \bar{a}(T) + \frac{\bar{b}}{4} \right], \quad (11a)$$

$$L(T) \equiv J_0(T) + \frac{3}{2} \frac{G_0(T)}{1 + \lambda} \left[\bar{a}(T) - \frac{\bar{b}}{2} \right]. \quad (11b)$$

The subscripts 0 indicate that strong-coupling corrections are not present. Another moment of $\alpha^2(\Omega)F(\Omega)$ giving strong-coupling corrections is defined as

$$\bar{c}(T) \equiv \int d\Omega \frac{2\alpha^2(\Omega)F(\Omega)}{\Omega^3} \ln^2 \left[\frac{1.13\Omega}{k_B T} \right]. \quad (12)$$

To find the specific-heat difference near T_c we use the solution of Eqs. (6) in (10) and obtain $t \equiv T/T_c$

$$\frac{\Delta c(T)}{\gamma T_c} = f + (1-t)g, \quad (13)$$

where

$$f = 1.43 \left[1 + a_1 \left[\frac{T_c}{\omega_{\text{ln}}} \right]^2 \ln \left[\frac{\omega_{\text{ln}}}{b_1 T_c} \right] \right] \quad (14a)$$

and

$$g = 3.77 \left[1 + a_2 \left[\frac{T_c}{\omega_{\text{ln}}} \right]^2 \ln \left[\frac{\omega_{\text{ln}}}{b_2 T_c} \right] \right]. \quad (14b)$$

Following Mitrović *et al.*,¹¹ the moments defined above can be written

$$\bar{a}(T_c) = \alpha_1 \frac{\lambda}{\omega_{\text{ln}}^2} \ln \left[\frac{1.13\omega_{\text{ln}}}{k_B T_c} \right], \quad (15a)$$

$$\bar{b} = \alpha_2 \frac{\lambda}{\omega_{\text{ln}}^2}, \quad (15b)$$

$$\bar{c}(T_c) = \alpha_3 \frac{\lambda}{\omega_{\text{ln}}^2} \ln \left[\frac{1.13\omega_{\text{ln}}}{k_B T_c} \right] \ln \left[\frac{1.13\omega_{\text{ln}}}{\beta_3 k_B T_c} \right]. \quad (15c)$$

α_1 , α_2 , α_3 , and β_3 are constants to be determined later through a phenomenological fit to the exact numerical results. a_1 , a_2 , b_1 , b_2 are simple functions of these constants. The average phonon frequency appearing in Eq. (15) is the Allen-Dynes¹⁹ frequency ω_{ln} . Furthermore, using the T_c equation of Leavens and Carbotte,¹⁶ we have

$$\frac{\lambda - \mu^*}{1 + \lambda} = \left[\ln \left[\frac{1.13\omega_{\text{ln}}}{k_B T_c} \right] \right]^{-1}. \quad (16)$$

Hence, the form of Eqs. (14) is obtained, where an inverse ln term has been dropped because its coefficient is estimated to be small. Note that no attempt is made to include strong-coupling corrections arising from γ . The exact results for f (the specific-heat jump) versus T_c/ω_{ln} are plotted in Fig. 1. Most of the electron-phonon spectral densities $\alpha^2(\Omega)F(\Omega)$ used come from the tabulation of Rowell, McMillan, and Dynes.²⁰ In each case the exact thermodynamics is obtained by full numerical solution of the Eliashberg equations (1) and (2) and the free-energy

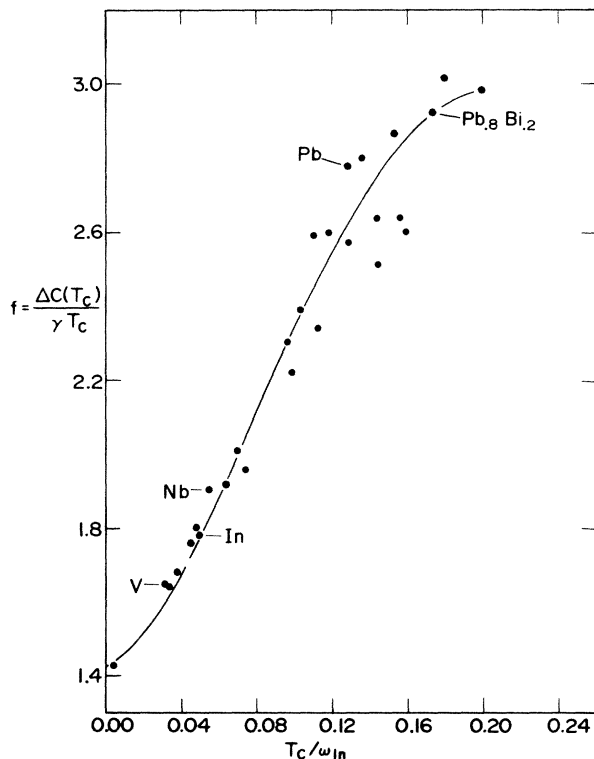


FIG. 1. Specific-heat-jump ratio $f \equiv \Delta C(T_c)/\gamma T_c$ vs T_c/ω_{ln} . The dots represent the accurate results from the full numerical solutions of the Eliashberg equations. In increasing order of $\Delta C(T_c)/\gamma T_c$ they correspond to the following systems: Al, Ta, V, Sn, Tl, In, $\text{Tl}_{0.9}\text{Bi}_{0.1}$, Nb (Butler), Nb (Arnold), Nb (Robinson), V_3Si , $\text{Nb}_{0.75}\text{Zr}_{0.25}$, $\text{Pb}_{0.4}\text{Tl}_{0.6}$, $\text{Nb}_3\text{Al}(2)$, V_3Ga , Hg, $\text{Nb}_3\text{Al}(3)$, $\text{Nb}_3\text{Ge}(2)$, $\text{Nb}_3\text{Ge}(1)$, $\text{Pb}_{0.6}\text{Tl}_{0.4}$, Nb_3Sn , $\text{Nb}_3\text{Al}(1)$, Pb, $\text{Pb}_{0.8}\text{Tl}_{0.2}$, $\text{Pb}_{0.9}\text{Bi}_{0.1}$, $\text{Pn}_{0.8}\text{Bi}_{0.2}$, $\text{Pb}_{0.65}\text{Bi}_{0.35}$, and $\text{Pb}_{0.7}\text{Bi}_{0.3}$. The dashed curve corresponds to $\Delta C(T_c)/\gamma T_c = 1.43[1 + 53(T_c/\omega_{\text{ln}})^2 \ln(\omega_{\text{ln}}/3T_c)]$. [See Eq. (18a) in the text.]

formula (9). Details are found in the literature.⁴⁻¹⁰ The values of ω_{ln} are mainly taken from the tabulation of Allen and Dynes.¹⁰ The results for the $A15$ compounds are taken from Mitrović, Schachinger, and Carbotte,⁹ and references cited therein. In determining the exact numerical results for the coefficient g in Eq. (13) (given in Fig. 2), we have used computed values of

$$D(t) \equiv \frac{H_c(t)}{H_c(0)} - (1 - t^2),$$

the critical magnetic-field-deviation function. Near T_c we expand

$$D(t) = \alpha(1 - t) + \beta(1 - t)^2. \quad (17)$$

From thermodynamic relations one can determine g from (17) in terms of α and β . The results for the coefficient g for a few selected materials are plotted in Fig. 2. In both Figs. 1 and 2 curves representing the formulas (14) have been drawn. The coefficients chosen are $a_1 = 53$, $b_1 = 3$ and $a_2 = 117$, $b_2 = 2.9$. Our final results are

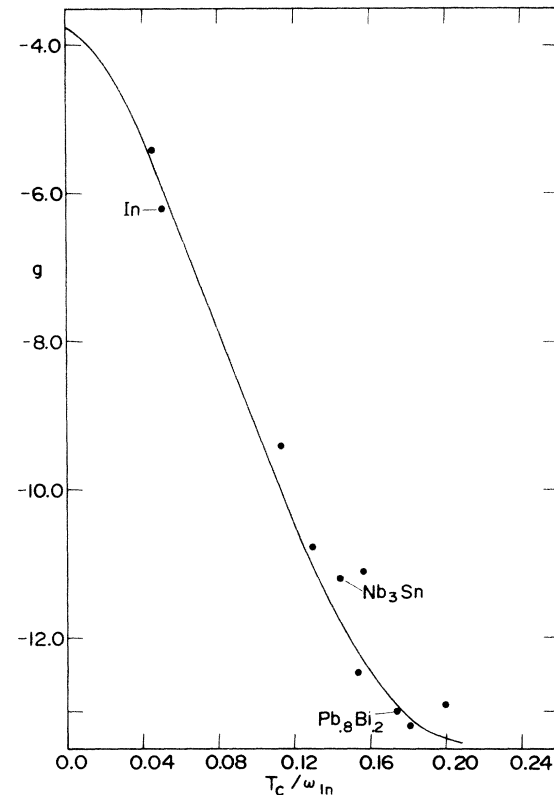


FIG. 2. Plot of g [see Eq. (13) in text] vs T_c/ω_{ln} for a selected number of systems. The dots correspond to results extracted from numerical solutions for $D(t)$ vs t , using the Eliashberg equations. The numerical values for g are obtained from $D(t)$ data. In decreasing order of g , the dots correspond to the following systems: Tl, In, $\text{Nb}_3\text{Al}(2)$, $\text{Nb}_3\text{Al}(3)$, $\text{Nb}_3\text{Al}(1)$, Nb_3Sn , $\text{Pb}_{0.9}\text{Bi}_{0.1}$, $\text{Pb}_{0.65}\text{Bi}_{0.35}$, $\text{Pb}_{0.8}\text{Bi}_{0.2}$, and $\text{Pb}_{0.7}\text{Bi}_{0.3}$. The dashed curve corresponds to $g = -3.77[1 + 117(T_c/\omega_{\text{ln}})^2 \ln(\omega_{\text{ln}}/2.9T_c)]$. See Eq. (18b) in the text. The fit is quite good, considering the constraints on the coefficients (see Sec. II).

$$f = 1.43 \left[1 + 53 \left(\frac{T_c}{\omega_{\text{ln}}} \right)^2 \ln \left(\frac{\omega_{\text{ln}}}{3T_c} \right) \right], \quad (18a)$$

$$g = 3.77 \left[1 + 117 \left(\frac{T_c}{\omega_{\text{ln}}} \right)^2 \ln \left(\frac{\omega_{\text{ln}}}{2.9T_c} \right) \right]. \quad (18b)$$

The coefficients in (18) were chosen phenomenologically; they could perhaps be improved upon slightly, but the improvement would be beyond the spirit of the approximations used to derive the form of Eqs. (18). We note in passing that the choices made agree reasonably well with estimates of the a_i and b_i based on the approximation $\alpha_i, \beta_i \approx 1$.

III. STRONG-COUPLING CORRECTION TO $\gamma T_c^2/H_c^2(0)$

To determine the correction to $\gamma T_c^2/H_c^2(0)$, we first determine the correction to $\Delta_0(0)$, the gap edge at zero temperature, starting with the imaginary axis equations (1) and (2). As T approaches zero, we use the well-known replacement²¹

$$\frac{1}{\beta} \sum_{m=-\infty}^{\infty} \rightarrow \int_{-\infty}^{\infty} \frac{d\omega}{2\pi} \quad (\omega_m \rightarrow \omega). \quad (19)$$

The approximation (5) becomes a step function on the continuous frequency axis, with a step at $\omega = \omega_0$. As before, we first consider ω small and $\omega \rightarrow \infty$, and obtain the strong-coupling corrections to the gap edge:

$$\Delta_0 = 2\omega_0 \exp \left[-\frac{1 + \lambda + \bar{\lambda}}{\lambda - \mu^*} \right] \times \left[1 + \frac{3}{2} \frac{\Delta_0^2}{\lambda - \mu^*} [\bar{a}(T_c) - \frac{5}{6}\bar{b}] \right]. \quad (20)$$

When combined with the T_c equation from Eq. (6), we find

$$\frac{2\Delta_0}{k_B T_c} = 3.53 \left[1 + a_3 \left(\frac{T_c}{\omega_{\text{ln}}} \right)^2 \ln \left(\frac{\omega_{\text{ln}}}{b_3 T_c} \right) \right], \quad (21)$$

where a_3 and b_3 are functions of α_1 and α_2 . Upon fitting Eq. (21) to numerical data, Mitrović *et al.*¹¹ found that the curve

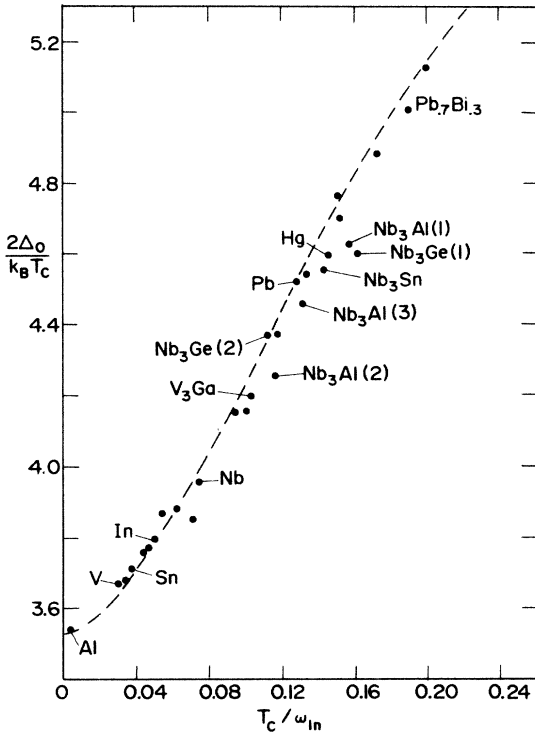


FIG. 3. The ratio $2\Delta_0/k_B T_c$ vs T_c/ω_{ln} . Most of the points have been reproduced from Ref. 11. We have also included recent numerical solutions of A15 compounds. In order of increasing $2\Delta_0/k_B T_c$, the dots correspond to the following systems: Al, V, Ta, Sn, Tl, $\text{Tl}_{0.9}\text{Bi}_{0.1}$, In, V_3Si , Nb (Butler), Nb (Arnold), Nb (Robinson), $\text{Pb}_{0.4}\text{Tl}_{0.6}$, $\text{Nb}_{0.75}\text{Zr}_{0.25}$, V_3Ga , $\text{Nb}_3\text{Al}(2)$, $\text{Nb}_3\text{Ge}(2)$, $\text{Pb}_{0.6}\text{Tl}_{0.4}$, $\text{Nb}_3\text{Al}(3)$, Pb, $\text{Pb}_{0.8}\text{Tl}_{0.2}$, Nb_3Sn , Hg, $\text{Nb}_3\text{Ge}(1)$, $\text{Nb}_3\text{Al}(1)$, $\text{Pb}_{0.9}\text{Bi}_{0.1}$, $\text{Pb}_{0.6}\text{Tl}_{0.2}\text{Bi}_{0.2}$, $\text{Pb}_{0.8}\text{Bi}_{0.2}$, $\text{Pb}_{0.7}\text{Bi}_{0.3}$, and $\text{Pb}_{0.65}\text{Bi}_{0.35}$. The dashed curve corresponds to $2\Delta_0/k_B T_c = 3.53[1 + 12.5(T_c/\omega_{\text{ln}})^2 \ln(\omega_{\text{ln}}/2T_c)]$. See Ref. 11 for a discussion of these results.

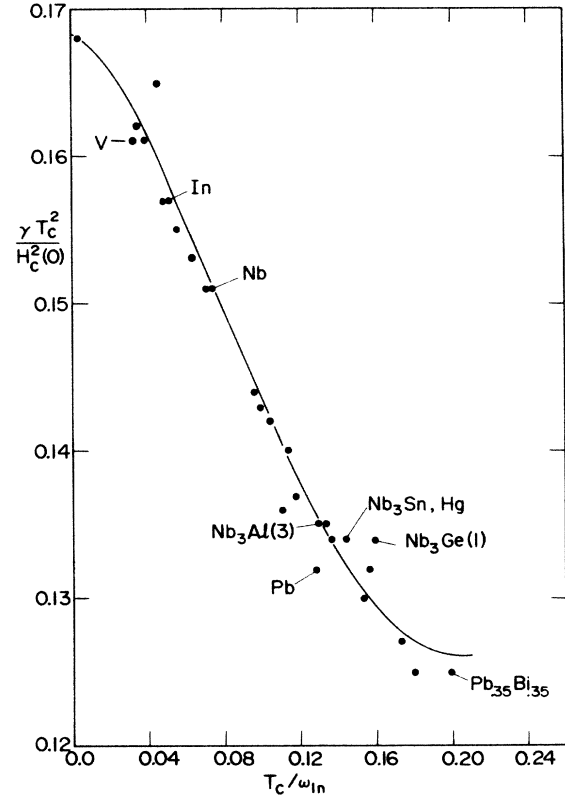


FIG. 4. The ratio $\gamma T_c^2/H_c^2(0)$ vs T_c/ω_{ln} . The dots represent results from the full numerical solutions to the Eliashberg equations. In decreasing order of $\gamma T_c^2/H_c^2(0)$, they correspond to the following systems: Al, Tl, Ta, V, Sn, In, $\text{Tl}_{0.9}\text{Bi}_{0.1}$, Nb (Butler), Nb (Arnold), Nb (Robinson), V_3Si , $\text{Pb}_{0.4}\text{Tl}_{0.6}$, $\text{Nb}_{0.75}\text{Zr}_{0.25}$, V_3Ga , $\text{Nb}_3\text{Al}(2)$, $\text{Pb}_{0.6}\text{Tl}_{0.4}$, $\text{Nb}_3\text{Ge}(2)$, $\text{Pb}_{0.7}\text{In}_{0.3}$, $\text{Nb}_3\text{Al}(3)$, Nb_3Sn , Hg, $\text{Nb}_3\text{Ge}(1)$, $\text{Pb}_{0.8}\text{Tl}_{0.2}$, Pb, $\text{Nb}_3\text{Al}(1)$, $\text{Pb}_{0.9}\text{Bi}_{0.1}$, $\text{Pb}_{0.8}\text{Bi}_{0.2}$, $\text{Pb}_{0.7}\text{Bi}_{0.3}$, and $\text{Pb}_{0.65}\text{Bi}_{0.35}$. The dashed curve corresponds to $\gamma T_c^2/H_c^2(0) = 0.168[1 - 12.2(T_c/\omega_{\text{ln}}/3T_c)]$. See Eq. (24) in text.

$$\frac{2\Delta_0}{k_B T_c} = 3.53 \left[1 + 12.5 \left(\frac{T_c}{\omega_{\ln}} \right)^2 \ln \left(\frac{\omega_{\ln}}{2T_c} \right) \right] \quad (22)$$

reproduced the general trend of the data quite well. A plot illustrating the numerical data as well as Eq. (22) is given in Fig. 3 (A 15-compound data has been added to the plot of Mitrović *et al.*¹¹).

To determine $\gamma T_c^2/H_c^2(0)$, we use Eq. (9) in the $T=0$ limit, with $Z_N(\omega)=1+\lambda$ for $|\omega| < \omega_0$ and again ignore the ω dependence in the logarithm. Using Eq. (21), we obtain

$$\frac{\gamma T_c^2}{H_c^2(0)} = 0.168 \left[1 - a_4 \left(\frac{T_c}{\omega_{\ln}} \right)^2 \ln \left(\frac{\omega_{\ln}}{b_4 T_c} \right) \right]. \quad (23)$$

Again, a_4 and b_4 are functions of $\alpha_1, \alpha_2, \alpha_3$, and β_3 ; they are chosen phenomenologically as $a_4=12.2$ and $b_4=3$. The curve

$$\frac{\gamma T_c^2}{H_c^2(0)} = 0.168 \left[1 - 12.2 \left(\frac{T_c}{\omega_{\ln}} \right)^2 \ln \left(\frac{\omega_{\ln}}{3T_c} \right) \right] \quad (24)$$

is plotted in Fig. 4, along with the numerical data. Equation (24) again fits the general trend quite well.

IV. CONCLUSIONS

Starting with the imaginary axis equations, several formulas [for the specific-heat jump, for the coefficient of the $1-t$ term in the specific-heat-difference expansion below T_c , for $2\Delta_0/k_B T_c$, and for $\gamma T_c^2/H_c^2(0)$] have been derived, giving strong-coupling corrections to the BCS predictions. We have taken a semiphenomenological approach and have fitted the correction coefficients to numerical data rather than evaluate the integrals requiring detailed information about $\alpha^2(\Omega)F(\Omega)$ for each material. The corrections required are all of the form

$$ax^2 \ln(1/bx), \quad (25)$$

where $x \equiv T_c/\omega_{\ln}$. While the methods used to obtain this result are quite new, this type of correction has already appeared in the literature for some time, namely in the work by Geilikman and Kresin,¹³ Kresin and Parkhomenko,¹⁵ and Geilikman *et al.*¹⁴ In this older work the appropriate phonon frequency appearing in (25) is not associated with ω_{\ln} of Allen and Dynes and the undetermined constants a and b are fixed in a very approximate way. Here they are obtained by consideration of exact numerical data obtained from solutions of the full Eliashberg equations for a number of materials with known electron-phonon spectral density. The values of the parameters a and b are given for the various cases in Eqs. (18), (22), and (24). The figures corresponding to these equations provide an idea of how well the formulas fit the numerical data. It is apparent that the general trend of the ratios is described very well by these approximate formulas. The formulas cannot, however, account for any deviations from the general behavior. In particular, functional derivatives based on such simple formulas for these ratios are qualitatively incorrect,²²⁻²⁴ as they depend on small differences.

If, however, an overall accuracy of 10% is acceptable, the formulas obtained should be useful in cases where the electron-phonon spectral density is not too different in shape from the typical shapes considered here. For oddly shaped spectra and higher accuracy it is necessary to go to numerical solutions of the complete Eliashberg equations.

A more detailed version of this paper describing many of the steps required to obtain the final formulas is available from the Physics Auxiliary Publication Source.²⁵

ACKNOWLEDGMENTS

This research was supported in part by the Natural Sciences and Engineering Research Council (NSERC) of Canada.

¹J. R. Schrieffer, *Theory of Superconductivity* (Benjamin, New York, 1964).

²See, for example, R. Merservey and B. B. Schwartz, in *Superconductivity*, edited by R. D. Parks (Dekker, New York, 1969), Vol. 1, p. 117.

³P. B. Allen and B. Mitrović, in *Solid State Physics*, edited by H. Ehrenreich, F. Seitz, and D. Turnbull (Academic, New York, 1982), Vol. 37, p. 1.

⁴D. J. Scalapino, in *Superconductivity*, Ref. 2, Vol. 1, p. 449.

⁵J. M. Daams and J. P. Carbotte, *J. Low Temp. Phys.* **43**, 263 (1981).

⁶J. M. Daams and J. P. Carbotte, *J. Low Temp. Phys.* **40**, 135 (1980).

⁷R. Baquero and J. P. Carbotte, *J. Low Temp. Phys.* **51**, 148 (1983).

⁸J. M. Daams, and J. P. Carbotte, M. Ashraf, and R. Baquero, *J. Low Temp. Phys.* **55**, 1 (1984).

⁹B. Mitrović and J. P. Carbotte, *Phys. Rev. B* **25**, 1244 (1982).

¹⁰B. Mitrović, E. Schachinger, and J. P. Carbotte, *Phys. Rev. B*

29, 6187 (1984).

¹¹B. Mitrović, H. G. Zarate, and J. P. Carbotte, *Phys. Rev. B* **29**, 184 (1984).

¹²C. R. Leavens and J. P. Carbotte, *Can. J. Phys.* **49**, 724 (1971).

¹³B. T. Geilikman and V. Z. Kresin, *Fiz. Tverd. Tela (Leningrad)* **1**, 3294 (1965) [*Sov. Phys.—Solid State* **7**, 2659 (1966)].

¹⁴B. T. Geilikman, V. Z. Kresin, and N. F. Masharov, *J. Low Temp. Phys.* **18**, 241 (1975).

¹⁵V. Z. Kresin and V. P. Parkhomenko, *Fiz. Tverd. Tela (Leningrad)* **16**, 3363 (1974) [*Sov. Phys.—Solid State* **16**, 2180 (1975)].

¹⁶C. R. Leavens and J. P. Carbotte, *J. Low Temp. Phys.* **14**, 195 (1974).

¹⁷J. Bardeen and M. Stephen, *Phys. Rev.* **136**, A1485 (1964).

¹⁸D. Rainer and G. Bergmann, *J. Low Temp. Phys.* **14**, 501 (1974).

¹⁹P. B. Allen and R. C. Dynes, *Phys. Rev. B* **12**, 905 (1975).

²⁰J. M. Rowell, W. L. McMillan, and R. C. Dynes (private com-

munication).

²¹A. A. Abrikosov, L. P. Gor'kov, and I. E. Dzyaloshinski, *Methods of Quantum Field Theory in Statistical Physics* (Dover, New York, 1975).

²²B. Mitrović, C. R. Leavens, and J. P. Carbotte, *Phys. Rev. B* **21**, 5048 (1980).

²³F. Marsiglio and J. P. Carbotte, *Phys. Rev. B* **31**, 4192 (1985).

²⁴G. Bergmann and D. Rainer, *Z. Phys.* **263**, 59 (1973).

²⁵See AIP Document No. PAPS PRBMDO-33-6141-33 for 33 pages of an expanded version of this paper giving some added mathematical detail. Order by PAPS number and journal reference from American Institute of Physics, Physics Auxiliary Publication Service, 335 East 45th Street, New York, NY 10017. The prepaid price is \$1.50 for a microfiche, or \$0.15 for a photocopy. Airmail additional.